# GPS-Denied Navigator for Small UAVs

# Final Report

University of Minnesota UAV Laboratory
Department of Aerospace Engineering & Mechanics
110 Union St, SE
Minneapolis, MN 55455
October 8, 2014

Authors:
Trevor Layh
Jordan Larson
Demoz Gebre-Egziabher
Brian Taylor
John Jackson
Yunus Agamawi

*The contents of this report reflect the views of the authors, who are responsible for the facts and the accuracy of the information presented herein. The authors acknowledge the United States Department of Homeland Security for supporting the work reported here through the National Center for Border Security and Immigration under grant number 2008-ST-061-BS0002. However, any opinions, findings, conclusions or recommendations in this paper are those of the authors and do not necessarily reflect views of the United States Department of Homeland Security.

# Contents

# List of Figures

# List of Tables

# Executive Summary

This report describes a recovery system for Small Unmanned Aerial Vehicles (SUAVs) operated in and around urban areas. The purpose of the system is to provide guidance so that the SUAV can navigate to a safe area where it can be recovered if GPS services are disrupted. The proposed system uses cell phone signals to bound the error growth of an air-data based dead reckoning system.

Currently, commercially available SUAV autopilots rely on a GPS-aided Inertial Navigation Systems (INS) to calculate the position, velocity, and attitude. However, GPS is known to be susceptible to interference and jamming. These vulnerabilities can be exploited, either intentionally or unintentionally, and cause GPS to become unavailable in a given geographical area. Consequently, the safety of SUAV operations can be compromised when operating in a GPS-denied region. Providing an alternative backup for or making GPS robust are indispensable requirements if SUAVs are to be routinely used in and around populated areas.

The prototype SUAV system presented in this report made use of a federated filtering approach to calculate position, velocity, and attitude in GPS-denied environments. Using measurements from an inertial measurement unit and magnetometer triad, an Attitude Heading Reference System (AHRS) Extended Kalman Filter (EKF) computed the attitude independent from the velocity and position. Using this attitude, an air-data based dead reckoning navigator provided a high-rate velocity and position solution. Periodic position fixes derived from cell phone signals were fused with the high-rate solution via a second EKF. Although future improvements to GPS backups may achieve performance that is comparable to GPS, the system presented is not capable of being as precise as GPS based navigation due to inaccuracies in the cell phone based positioning method utilized. Nevertheless, the purpose of the system is not to provide an accurate navigation solution per se but to guide the SUAV to a location where a safe manual or automatic recovery of the aircraft can be accomplished.

The cell phone based positioning is derived from timing advance (TA) data provided via cell tower communications with an onboard receiver. These TAs can be translated into time-of-arrival (TOA) and subsequently into range estimates between the tower and receiver. However, the TAs currently available on cell phone networks are discretized into time lengths defined by bit periods which are 48/13 µs. Consequently, the range estimates have effectively been discretized into 553.46 m increments originating from the cell tower location.

Several flight tests were completed to compare the results of a traditional GPS-aided INS, an un-aided dead reckoning system, and the cell phone-aided system. Due to the limitation of discretized TAs coupled with limited airspace for testing, a hardware-in-the-loop (HIL) simulation was developed to illustrate system performance during extended GPS outages. After validating and verifying the HIL simulation, three Monte Carlo simulations demonstrated that the cell phone position estimates bound the drift encountered by an un-aided dead reckoning system. After navigating without GPS for fourteen miles, the average position error on the un-aided dead reckoning solution was 6765 m compared to only 200 m for the cell phone-aided system. Thus, this performance demonstrates that the system accomplishes the design objective of guiding the SUAV to a safe location for recovery of the aircraft.

In closing, future design improvements which are expected to enhance the systems performance are discussed. These improvements include developing a software defined cell phone receiver to yield more accurate TOA measurements as well as incorporating cell phone Received Signal Strength Indication (RSSI) as an additional measurement.

# 1 Introduction

To date, Small Unmanned Aerial Vehicles (SUAVs) have been used most extensively in military operations. However, many non-military applications for these vehicles exist including important law enforcement and civilian uses. Additionally, the Federal Aviation Administration (FAA) Modernization and Reform Act of 2012 (HR658) requires the FAA to integrate routine unmanned aircraft operations into the national airspace system (NAS) as quoted from Section 332 "as soon as practicable, but not later than September 30, 2015." Consequently, the abundance of everyday tasks that UAVs can complete with precision and repeatability coupled with interest from both government and commercial entities alike to safely integrate these vehicles into the NAS for expanded use has lead to a number of issues that still need to be addressed. Some of the most critical of these issues include concerns of privacy, cost, reliability, and liability. The focus of this white paper we will be on the reliability of the navigation system used in UAVs.

Some of the vulnerabilities that threaten Global Positioning System (GPS) signals will be presented, and the critical role that GPS plays in allowing a SUAV to safely and accurately complete its tasks. After summarizing several potential backup systems for GPS, we will present a navigation system design that relies on an auxiliary source of positioning information derived from cell phone signals and its performance in a nominal SUAV environment. It is important to note that is unlikely that any backup system will provide the same level of accuracy as GPS currently does. Although it is possible that future improvements may deliver an alternative to GPS that provides comparable accuracy, waiting for such a development would unnecessarily delay the benefit SUAVs can provide law-enforcement units today. In our opinion, the backup system should be viewed as a system that will allow the SUAV to navigate out of a GPS-denied region to its home base or other safe location. Therefore the design presented in this paper was developed to provide a backup navigation system allowing the SUAV to safely "limp back home". This is in contrast to an alternative position system capable of allowing extended SUAV operations with or without GPS services.

Before describing the system developed in this work, for completeness, background material is provided to help put the results into context. To this end, the following sections present the motivation for this work; describe SUAV flight control system guidance, navigation, and control operations; GPS vulnerabilities; and mitigation techniques. A more detailed background on the impacts and mitigations of GPS-unavailability in SUAVs can be found in [1].

## 1.1 Motivation

There are several envisioned applications for UAVs, and as mentioned, one of the areas of interest include law-enforcement agencies. These organizations are entrusted with several critical tasks in which UAVs can improve mission performance. For this work, we focused on SUAVs weighing under 20 lbs which fall within the "Class I" category as defined in [2]. Some of the tasks that can be fulfilled or in some way augmented by SUAVs include operations such as reacting to an unforeseen security threat, where quick and accurate information is required for effective decision making. An SUAV can be equipped with a variety of sensors (Electro-Optical, Infrared, microphone, etc.) that can enhance situational awareness. The real-time information provided by these sensors can be relayed through a SUAV ground control operator to the law-enforcement units reacting to the threat. Other tasks may be more repetitive day-to-day procedures such as surveillance in remote or hard-to-reach areas (i.e. border patrol operations). Additionally, SUAVs can be used to aid in search and rescue missions, emergency and natural disaster response, and damage assessments. One recent example of these types of applications include the 2011 disaster at Japan's Fukushima Daiichi nuclear facility where the Honeywell T-Hawk gathered up-close video and photos inside the plant in an effort to limit radiation releases [3].

Unmanned Aerial Systems (UAS) refers to the entire system that consists of the air vehicle, data link, ground station, and additional support equipment. Due to the small size of SUAVs, they typically have very little support equipment required and some are small enough to fit in the trunk of a car allowing for easy transportation. One attribute of these UAS that improve overall mission performance is that their operational requirements reduce the human resources necessary to complete an objective. These vehicles are capable of remaining on station for extended periods of time without the need to refuel in the case of gas-powered, or similiar, vehicles. In most cases, battery-powered vehicles have limited flight plans due to recharging requirements, but advancements in battery technology will almost certainly reduce these limitations. Another reduction on human resources is that UAVs are not constrained by the crew rest requirements of manned aircraft. This is because unmanned operations afford the flight crew the opportunity to rotate operators throughout a mission which can allow for sustained coverage of surveillance areas for long periods of time. Finally, these advantages are in addition to the obvious reduction in risk of personnel loss should a mishap occur.

## 1.2 Guidance, Navigation, and Control

In order for a SUAV to autonomously complete a task or mission, the onboard computer or autopilot must perform the key tasks of guidance, navigation, and control (GNC). The vehicle's position, velocity, and attitude (orientation) are essential for GNC. Commonly referred to as the vehicle's *navigation state* or *state*, these three quantities are estimated by the SUAV's navigation and attitude determination algorithms by utilizing the sensors available on the aircraft. Figure 1 shows a block diagram of the interactions between the guidance, navigation, and control systems and their ground station and onboard sensors.

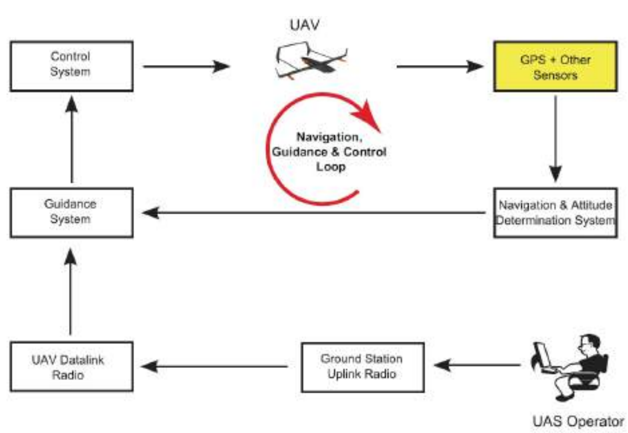


Figure 1: Block Diagram of UAV Autopilot Navigation, Guidance, and Control Loop (Reproduced from [1])

The guidance system uses the estimate of the SUAV's state to define a safe path to the mission's goals as instructed by the operators from the ground station. For example, the guidance system uses the estimates for position to determine the course necessary to complete a way-point route, and the attitude estimates to maintain a specific heading and a constant attitude. A control system will then make use of the SUAV's current velocity and attitude to decide how to manipulate the aircraft's control surfaces and throttle to track the safe path determined by the guidance system.

This block diagram illustrates the importance of navigation and attitude determination systems. GPS is a critical sensor for accurate position and velocity measurements. Although multiple GPS receivers with adequately spaced antennae can be used to determine attitude, most SUAVs are not large enough for this approach. Consequently, a widely accepted and proven method for attitude determination for smaller UAVs is to combine the GPS sensor with an Inertial Navigation System.

## 1.3 GPS-aided Inertial Navigation Systems

Inertial Navigation Systems (INS) provide vehicle position and orientation estimates using an Inertial Measurement Unit (IMU) to measure accelerations and rotation rates. Unlike GPS, IMUs do not require a radio frequency (RF) connection to an outside signal. Instead, all IMU measurement signals are self-contained which makes them very useful in nearly all environments including indoors and underwater as well as in open air. Despite this capability of operating in any environment, low-cost IMUs cannot obtain the same level of precision as GPS sensors, which can provide meter-level position accuracy and sub-decimeter per second velocity measurements. The lack of accuracy in low-cost IMUs is caused by inherent errors in the measured accelerations and rotation rates which lead to drift in position and velocity with time. SUAVs require components that are small and light with low power requirements, and therefore, typically "automotive" grade Micro-Electro-Mechanical Systems (MEMS) IMUs are installed in these small aircraft. Table 1 shows a rough guide for the INS error growth rates and costs associated with IMUs at four quality grades and illustrates that although all IMUs exhibit drift, the errors are considerably higher in lower-cost units.

| **Quality Grade** | **Position Error Drift Rate (km/hr)** | **Approximate System Cost** | **Typical Applications** |
|---|---|---|---|
| Strategic Grade | less than 0.001 | \$10,000,00+ | Submarines, ICBM |
| Navigation Grade | 1.5 | \$50,000 - \$100,000 | Aircraft Navigation |
| Tactical Grade | 20-100 | \$10,000 - \$20,000 | Smart Munitions |
| Automotive Grade | 100+ | \$100 - \$10,000 | Cars, UAVs, Toys |

Table 1: INS/IMU Quality Grade and Drift Rates (Reproduced from [1])

This drift of approximately 100+ meters/minute in automotive grade components is far to large to be tolerated. Therefore, it is imperative that this drift be corrected by "resetting" the INS with some other navigation sensor or external information. To accomplish this, practically all SUAV autopilots employ a GPS-aided INS as the navigation system. The GPS position and velocity information can be used to periodically reset the position and velocity estimates derived by the INS alone. Attitude can be determined by the INS, but by utilizing an extended

Kalman filter (EKF), the GPS and INS sensors can be fused to indirectly correct for errors in the attitude, velocity, and position which yields a drift free estimate of the entire navigation state. Figure 2 displays the typical architecture of a GPS-aided INS.

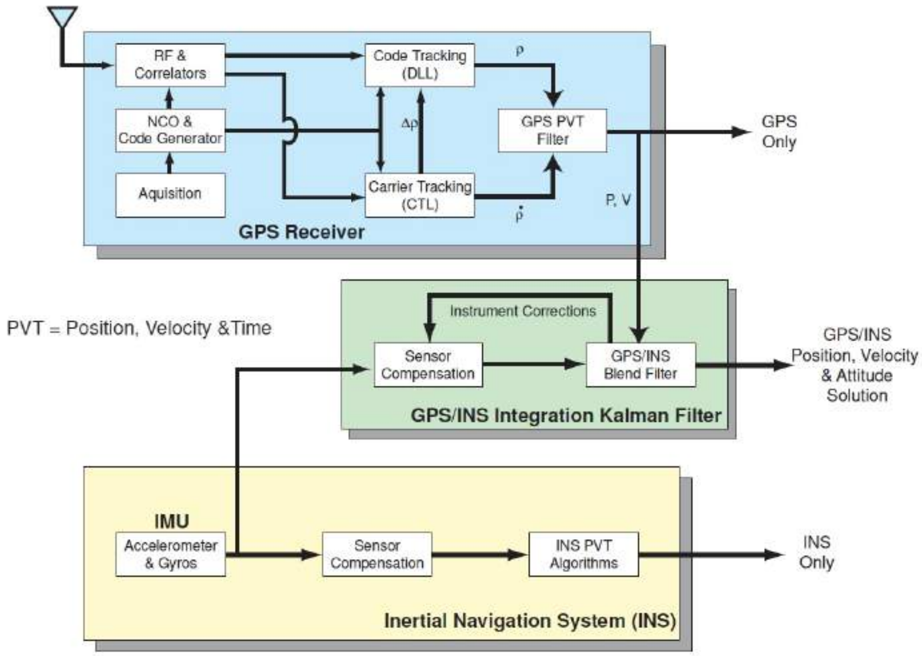


Figure 2: Typical Architecture of a GPS-Aided INS Found in Most SUAV Autopilots (Reproduced from [1])

As indicated by the architecture in Figure 2, the GPS position and velocity estimates are critical to arrest the error growth in the INS-only solution. However, there are a number of GPS vulnerabilities that exist and, if encountered, can cause intermittent loss of GPS signals or even a complete GPS-denial. Thus, it is paramount that an SUAV is either capable of avoiding nearly all GPS vulnerabilities or be equipped with a backup capable of bounding the errors created by INS only solutions during GPS disruptions.

## 1.4 GPS Vulnerabilities

GPS is a Global Navigation Satellite System (GNSS) maintained and operated by the United States Department of Defense. GNSS is a broader term to encompass all versions of global navigation systems reliant upon satellites. The Russian Federation's GLONASS, European Union's Galileo, China's Compass/Beidou, and Japan's regional system Quasi-Zenith are also GNSSs. While these vulnerabilities and the research discussed in this paper focus on GPS, the concepts presented are equally applicable to all GNSS systems. This is due to all GNSS systems being capable of providing relatively comparable performance, operating with the same basic design principles, and emitting on similar frequencies.

GPS uses a constellation of Medium Earth Orbit (MEO) satellites which broadcast a continuous signal modulated on two L-band radio-frequency carriers, $L_1$ at 1575 MHz for civilian users and $L_2$ at 1227 MHz for DoD authorized users. The positions of the GPS satellites are precisely known, and a user can accurately determine their position by processing the ranging signals from at least four of the satellites due to the user needing to solve for four unknowns (latitude, longitude, altitude, and time). The GPS satellites orbit at approximately 20,000 km above the surface of the Earth, and therefore, the signal power observed by a user on Earth is limited to -160 dBW due to the large distance traveled and area covered by the signal. This low signal power means the GPS signal is below the ambient background noise of many places on Earth where GPS is used most. Although GPS receivers are designed to extract this low power signal out of the ambient noise and process it, relatively small increases in the magnitude of the ambient noise can reduce the ability of GPS receivers to extract all the information from the signal. In addition to this, even if the ambient noise remains unchanged, it is possible for the GPS signals to be attenuated prior to their reception by the user. The correct operation of the GPS signal processing in the receiver relies upon the proper determination of the transit time for the signal to travel from the satellite to the user. Thus, small deviations due to radio frequency interference (RFI) from other RF signals at the same frequency or obstructions caused by buildings, trees, etc. can lead to inaccuracies in the position solution and compromise the ability of the receiver to track the satellite's signal.

The attenuation caused by buildings or trees, although difficult to correct for within the receivers or autopilot, can be avoided in most SUAV applications by skillful mission planning to fly at an altitude appropriate to avoid obstructions. Flight profiles requiring navigation through obstacles such as the urban canyons of a large city would require an alternative or backup navigation sensor capable of arresting the errors accumulated by a low-cost INS. The case of interfering radio signals is much more complicated and is not as easily avoided by mission planning. Due to the availability of only one carrier for civilian users and whether intentional or unintentional, GPS interference has ability to stress and even deny GPS for all users within the affected area. This fact was demonstrated, albeit unintentionally, in January of 2007 in San Diego, California when a US Navy training exercise in communications jamming between two ships in the area accidentally denied GPS services for a large portion of the city [4]. Intentional jamming using relatively cheap equipment can produce similar outages to GPS as described in [4] where a truck driver, who didn't want his employer knowing where he was, used a jammer that caused GPS interruptions at Newark airport in New Jersey. Additionally, a GPS outage encountered by a UAV which led to a fatality is described in [5].

In addition to RFI, another vulnerability is GPS-spoofing, which is an attack whereby a malicious entity generates a GPS-like signal designed to mislead GPS receivers. The goal of GPS-spoofing is to make a user's GPS receiver "believe" that it is located somewhere other than it's actual position. This vulnerability was demonstrated to the U.S. Department of Homeland Security in June 2012 by researchers from the University of Texas at Austin where the research team repeatedly overtook navigational signals going to a GPS-guided SUAV [6]. DoD authorized users of GPS have access to a spoof-resistant signal. Thus, these users are more difficult to hack and therefore less vulnerable to GPS-spoofing attacks than civilian users. Procedures for managing GPS-spoofing as well as RFI will be addressed in the next section.

## 1.5 Methods for Handling GPS Vulnerabilities

For the approaches to handling the various GPS vulnerabilities, we will categorize the methods by the environment (GPS-stressed, GPS-spoofed, or GPS-denied) that they are designed to mitigate. GPS-stressed environments are characterized by an RFI that reduces but does not completely suspend the ability of a receiver to accurately track the GPS signal being transmitted by the satellite. The results of these types of environments will be intermittent GPS position solutions that may or may not be accurate. The characteristics and effects of a GPS-spoofed environment were described in the previous section. GPS-denied environments, as the name implies, are those where a receiver is unable to track the GPS signals altogether. In these environments, no receiver will be able to track a GPS signal, and if the interference cannot be located and eliminated, a backup navigation system must be employed.

One technique for dealing with a GPS-stressed environment is to use *vector tracking* GPS receivers rather than the conventional *scalar tracking* GPS receiver. Scalar tracking independently tracks each satellite's signal by a single channel dedicated to that satellite. Therefore each channel performs the operations of signal acquisition, tracking, and data demodulation with no information exchange between the channels. Vector tracking receivers simultaneously track all satellites that are visible to the receiver using an estimator such as an Extended Kalman Filter. This simultaneous processing approach has been shown to improve performance in GPS-stressed environments since signals that have been attenuated by RFI can be aided by information from the other satellites. Likewise if all satellite signals received are interfered, the fusion of all the signals can provide an increased accuracy of position information over traditional scalar tracking receivers in the same environment.

Although GPS-spoofing a receiver on a SUAV is possible, countering such an attack is relatively straight-forward as has been demonstrated as referenced in [1]. The most effective mitigation of GPS-spoofing is to take advantage of the fact that it is difficult to simultaneously spoof multiple users who are capable of communicating with each other. A system such as that described in [7] can be used to protect against spoofing attacks by periodically sending GPS signals received to a trusted authenticator. The authenticator could then make use of watermarks that exist within the GPS signal to determine if the signal is legitimate.

As mentioned before, GPS position and velocity information is vital for a SUAV's flight control system to carry out the guidance, navigation, and control of the aircraft. Therefore, mitigations of a complete GPS denial scenarios are among the most critical for the safe operation of a SUAV that employs a GPS-aided INS. During periods of GPS denial, a secondary/back-up navigation system must replace GPS. A potential replacement for the architecture of a GPS-aided INS as shown in Figure 2 is displayed in Figure 3.

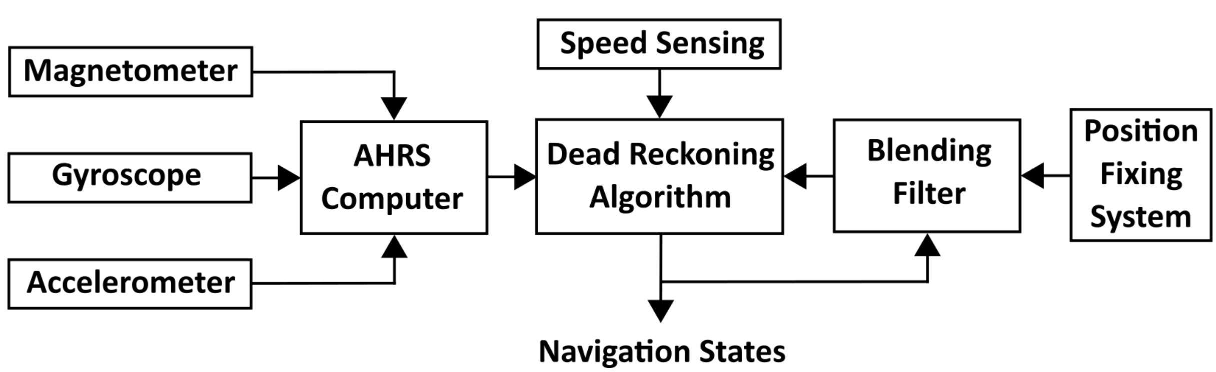


Figure 3: System Architecture of a GPS-Backup Dead Reckoning Navigator (Reproduced from [1])

This dead reckoning system makes use of airspeed measurements, a backup position fixing system, and an Attitude Heading Reference System (AHRS) to calculate the SUAV's navigation state vector. The source of the airspeed and other measurements needed for the dead reckoning system as well as a description of how the AHRS determines the attitude will be discussed in more detail later in Section 3.2. As described in [1], there are several potential sources for Alternative Positioning, Navigation, and Timing (APNT) to take over when GPS is unavailable, and we will briefly summarize three of these sources.

### 1.5.1 Vision-Based Navigation

Vision-based navigation makes use of images taken by a digital camera to determine position and orientation. Although, the size, weight, and power requirements of SUAVs will not allow for high rate vision-based solution, an INS or dead reckoning system can provide the high-rate solution while the vision-based solution would supply periodic updates to correct the drift of the high rate solution. One method of vision-based navigation operates by requiring a previously prepared reference image with a library of geo-tagged visually distinct landmarks uploaded to the aircraft. During flight, "just-captured" images by the onboard camera would be compared to the distinct landmarks against those on the reference image to determine the position of the aircraft. A second method would not require a previously uploaded reference image, but instead the reference image would be the first image taken during flight when GPS is available. Therefore, aircraft position and attitude are known for the reference image and subsequent images can be compared to the reference to determine position and attitude. However, neither of these methods are all-weather solutions since they require an unobstructed view of the ground. While vision-based navigation has been developed and matured for terrestrial robotics, further study is needed for UAV applications.

### 1.5.2 Cooperative Navigation

Another back-up is cooperative navigation which would, in some respects, operate in a similar way to GPS satellites and receivers whereby a radio transceiver on another SUAV, law enforcement vehicle, or static tower could act as a *collaborator* with the distressed SUAV also equipped with a radio transceiver. The distressed SUAV (position unknown) would send an interrogation signal to the collaborator (position known) which would enable range measurements derived from round-trip timing. The cooperative nature of this method is simultaneously its greatest strength and weakness. Since the only requirement is installing the correct hardware for communication, cooperative navigation is easily scalable and very flexible. However, it requires active cooperation thereby limiting navigation to areas where collaborators exist.

### 1.5.3 Signal of Opportunity Navigation

A third type is Signal of Opportunity (SOP) navigation which uses any and all signals available to determine a solution. SOPs can include signals designed for AM radios, FM radios, or HDTVs. Due to the increasing number of radio-frequency signals, SOP navigation can be a viable alternative especially since there should be little to no infrastructure cost for the user. However, the research and development work in this area is only just beginning and much more work needs to be done.

A SOP technique, which is the focus of this work, is positioning based on cell phone signals. Signals from cell phone towers can be used to develop a map of a given area in terms of the Received Signal Strength Indicator (RSSI) values observed by a cell phone receiver from all towers that are visible. This mapping, commonly referred to as RF *fingerprinting*, is performed while GPS positioning is available. Then, when GPS is unavailable, the signal strength map is referenced by a machine learning algorithm as the receiver picks up new cell phone signals. One significant drawback to this method is if the SUAV flys into a GPS-denied region that has not been mapped, then a position solution cannot be obtained. In addition to the fingerprinting method, a traditional multi-lateration approach can be used if cell phone tower positions, signal time of arrival (TOA), and/or signal direction of arrival are known. However despite very good cell phone coverage in urban settings, rural areas are not as well served, and it may be more difficult to obtain accurate positioning in these areas using cell phone signals only. In this paper, we will detail the setup and performance of using a multi-lateration approach with available cell phone signals for SUAV navigation.

## 1.6 Problem Statement and Paper Organization

Despite the numerous benefits that UAVs can provide to law-enforcement operations, one of the major limitations of these vehicles is their high accident rate relative to manned aircraft. There are many causes for this including the fact that UAV technology is still relatively new and evolving. Additionally, a critical characteristic of UAVs, and SUAVs in particular, is their low-cost which encourages the use of commercial-off-the-shelf (COTS) components. The limited reliability of low-cost hardware corresponds to a reduction in reliability of the overall system and increases failure probability. The high accident rate reduces safety and is therefore one of the major obstacles to integrating UAVs into the NAS. One method, proven in commercial aircraft applications, for improving reliability is increasing the hardware redundancy of various aircraft systems which are most susceptible to failures. However, this approach inevitably leads to higher cost and consequently reduces one of the most attractive characteristics of SUAVs.

In this paper, we will focus on the reliability of a SUAV navigation solution which heavily depends on GPS for proper functioning. This dependence on GPS means that GPS vulnerabilities translate into SUAV vulnerabilities, and hardware redundancy alone will not mitigate these issues since interference of one GPS receiver will affect all onboard GPS receivers. In this paper, we propose a cell phone based substitute to GPS for aiding the SUAV's guidance, navigation, and control systems.

With this mind, the remaining sections of this paper are organized in the following manner. In the next section, we will describe one possible situation and environment in which a SUAV may be used and encounter a GPS interruption requiring activation of the backup system. Section 3 will summarize the hardware used for the construction of the SUAV utilized in this research. Additionally, the software of the cell phone-aided navigation filter will be discussed explaining the derivation of the range measurements extracted from cell phone signals as well as the navigation and attitude determination system aided by these measurements. Next, the setup and results of flight testing the backup system will be reviewed and illustrated in Section 4. Due to the combined limitations of the system and available flight area, simulation results will also be used to expand the analysis of the system's performance, but only after validating and verifying the hardware-in-the-loop simulation behaves in a similar manner to real flight tests. Finally, we will address some of the limitations, mitigations, potential improvements, and future work related to the cell phone-aided navigation system.

## 2 Concept of Operations

The system developed is designed to provide a backup navigation solution to a SUAV flight control system when GPS is unavailable. The flight area is assumed to have cell phone tower coverage whereby the onboard cell phone receiver has line-of-sight communications with at least two cell phone towers for at least 50% of the time during the flight. This secondary system will be capable of allowing the SUAV to navigate out of a GPS-denied environment and return to base. Due to the limitations of the system, which will be detailed in Section 4, the proposed back-up will not be capable of providing the same level of accuracy as GPS. Instead, the system will safely navigate the aircraft back home where there is either GPS available for an auto-landing, or the SUAV is capable of being landed on manual control by the SUAS pilot. Therefore, we also anticipate that the aircraft will be initialized and operating in its assigned area for some time with GPS available.

As will be shown in Section 4, the backup system will be capable of maintaining small errors on altitude; however, the errors in latitude and longitude will limit the aircraft's ability to avoid obstacles such as trees, buildings, etc. that are at the same relative altitude as the SUAV. Therefore the nominal environment in which this system would provide a safe transition back home would be one whose flight plan would keep the aircraft at a higher altitude than any obstacles within the mission area. Figure 4 depicts a nominal scenario where a SUAV is assisting in emergency response which is far from the base station. Additionally, this scenario places the SUAV outside the range of any direct manual control of the aircraft by a remote pilot. Thus, requiring the flight control system to autonomously guide the aircraft back to its home base. Figure 4 shows the period of time when GPS is available. At some point during the mission GPS services are interrupted by a jammer, as shown in Figure 5, and the backup system will take over navigating the aircraft and guide it back to the base station where a safe manual or automatic recovery of the aircraft can be accomplished.

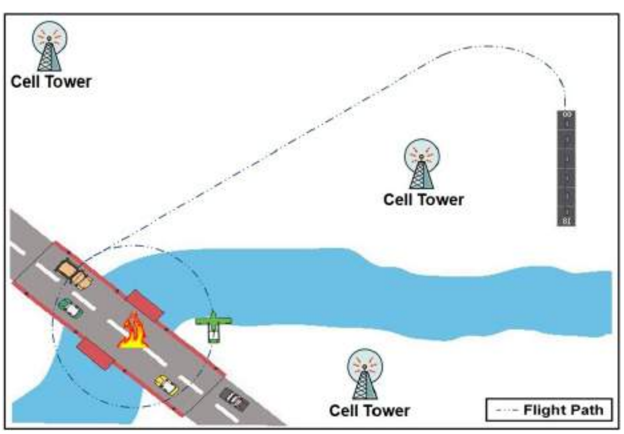


Figure 4: Cell Phone Navigation Scenario when GPS Available

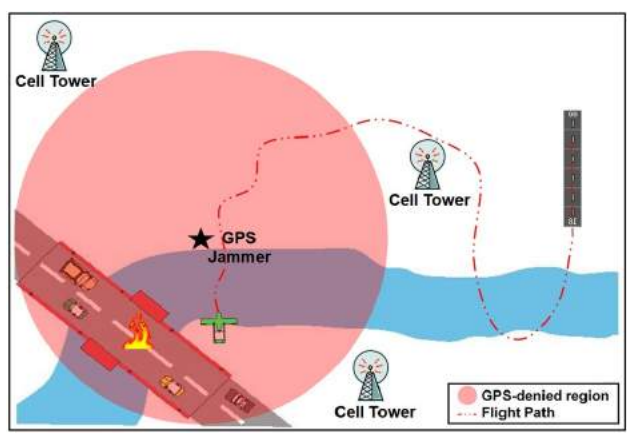


Figure 5: Cell Phone Navigation Scenario when GPS Unavailable

Upon determining that GPS is no longer reliable, the SUAV flight control system will begin using data obtained from an onboard cell phone modem containing time of arrival information from a subset of the cell phone towers in view of the receiver. This cell phone data will be fused with the information from other onboard sensors in a filter to aid a dead reckoning navigation system.

# 3 System Architecture

The cell phone-aided dead reckoning navigator uses an AHRS to determine the attitude of the aircraft. The attitude solution from the AHRS is fused with air data measurements to mechanize a dead reckoning system to estimate the position and velocity of the aircraft. Since an accurate estimation of attitude is crucial for the control laws of the aircraft to maintain stable flight, this cascaded approach allows for an independent estimation of the attitude of the aircraft. The separation of the attitude and position estimates is in contrast to a traditional GPS-aided INS filter. Furthermore, this cascaded-filter approach will prevent the relatively large position errors inherent in the cell phone data from corrupting the attitude solution. This system architecture, shown in Figure 6, makes use of two separate filters, one for the AHRS and one for the dead reckoning, which will be discussed in detail in Section 3.2.

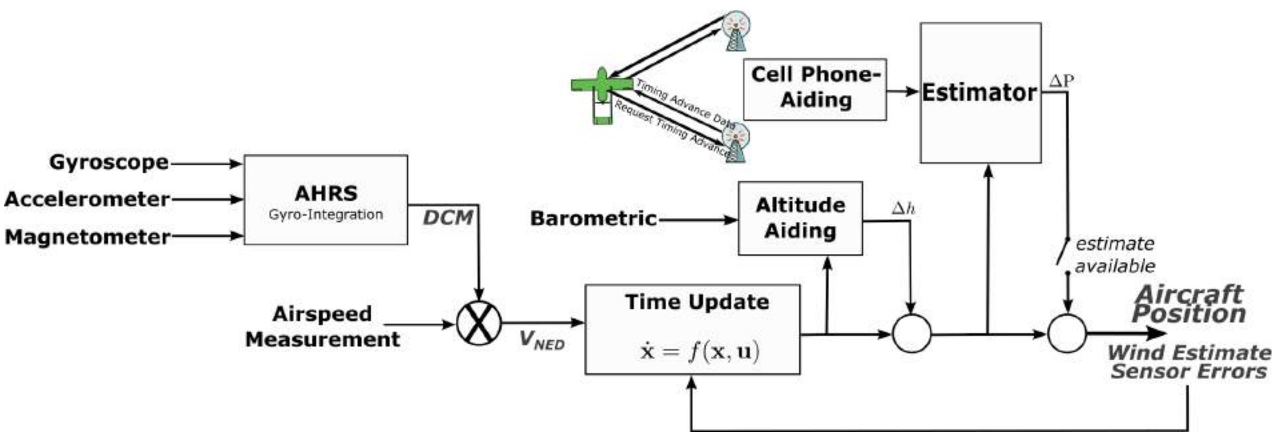


Figure 6: Cell Phone Navigation System Architecture

This backup system was integrated into the University of Minnesota UAV Research Group (UMN-URG) Goldy flight control system. An overview of the hardware and software used in the standard Goldy FCS is given as well as the necessary additions made to support the cell phone modem used for this research.

## 3.1 Hardware

The cell phone navigation system was implemented onto the Goldy FCS and flown on an UMN-URG research vehicle built specifically for this work. The aircraft, shown in Figure 7, is an Ultra Stick 25e whose specifications are listed in Table 2.

Figure 7: Ultra Stick 25e

| Parameter | Value |
|---|---|
| Mass | 1.959 kg |
| C.G. from Firewall | 0.222 m |
| Aero Ref from Firewall | 0.2175 m |
| Ixx | 0.07151 kg*m$^2$ |
| Iyy | 0.08636 kg*m$^2$ |
| Izz | 0.15364 kg*m$^2$ |
| Ixz | 0.014 kg*m$^2$ |
| Chord | 0.25 m |
| Span | 1.27 m |
| Wing Area | 0.3097 $^2$ |

Table 2: Ultra Stick 25e Specifications

The customized Goldy FCS is shown in Figure 8. It is equipped with a sensor suite that includes an IMU, GPS receiver, and two pressure sensors. The pressure sensors in addition to the pitot tube and plumbing form the pitot-static system. In addition the system uses a cell phone modem to provide periodic position fixes. Table 3 gives a list of the individual components used to mechanize this backup navigation system. This air vehicle along with every component in the Goldy FCS is available commercially off-the-shelf (COTS) and was chosen for capability as well as maintaining the low-cost objective of SUAVs. Further details related to the Ultra Stick 25e, the Goldy FCS, and other UMN-URG equipment can be found in [8].

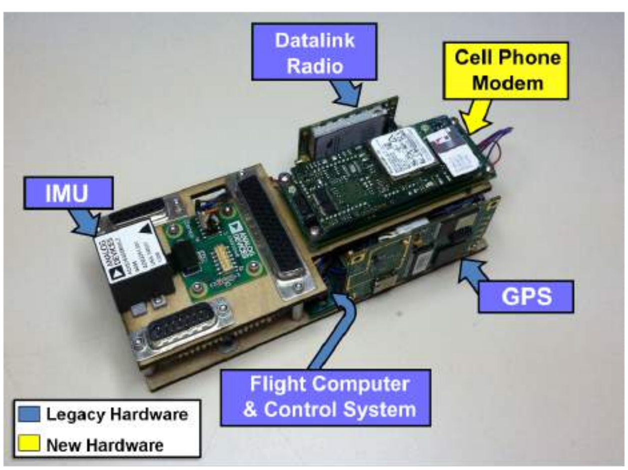


Figure 8: UMN-URG Goldy Flight Control System

| Component | Manufacturer Product |
|---|---|
| Inertial Measurement Unit (IMU) | Analog Devices ADIS 16405 |
| GPS Receiver | Hemisphere Crescent OEM Board |
| Datalink Radio | Freewave MM2 900 MHz |
| Flight Computer | Phytec MPC5200B Tiny |
| Pressure Transducers | AMSYS AMS5812 |
| Cell Phone Modem | Multi-Tech Systems MT100EOCG-G2 |

Table 3: UMN-URG Goldy FCS Components

The cell phone modem used for this research was made by Multi-Tech Sytems [9]. The Open Communications Gateway - Embedded (OCG-E) product was chose for its COTS availability as well as its low weight, cost, and power requirements. Additionally, the OCG-E's small footprint allowed for integration within the Goldy FCS and the SUAV. The MT100EOCG-G2 variant was chosen because of its unique capability to request the Cell Environment Description (+CCED) command from the main serving cell phone tower as well as up to six neighboring towers. This +CCED command is unique in that it supplies the modem with timing advance (TA) data for each of the available towers organized by their Cell ID (CID). CID is a unique number used to identify each tower within a given cell phone provider's network.

### 3.1.1 Cell Phone Modem Operation

As described in [10], the TA is a signal sent by a cell phone tower to the cell phone receiver. The TA is used by the receiver to compensate for propagation delay when communicating with the tower. The expected time delay from a signal being sent by a receiver to a tower is zero when the tower and the cell phone are collocated. These TAs are measured in bit periods, rounded to the nearest whole bit period, and are thus accurate to $\pm 1$ bit period. A bit period is 48/13 µs in length. The TAs are equal to the round trip time for a signal sent from a tower to be received by the receiver and sent back to the tower. This TA data is then sent to the modem upon request via the +CCED command.

Because these TAs are rounded to the nearest bit period, this yields the following resolution for the cell phone modem range measurement given the speed of light is $2.997\,924\,58 \times 10^8\ \frac{\text{m}}{\text{s}}$:

$$\text{1 Bit Period } = \left(\frac{48}{13} \times 10^{-6}\,\text{s}\right)\left(2.997\,924\,58 \times 10^8\,\frac{\text{m}}{\text{s}}\right)\left(\frac{1}{\text{2 trips}}\right) = 553.46\,\text{m} \tag{1}$$

Thus, one significant drawback is that the range measurement can be in error by as much as 553.46 m. This does not include additional noise or error sources on the TA data due to multi-path effects or RFI on the cell phone signals. Figure 9 frames this issue in another way.

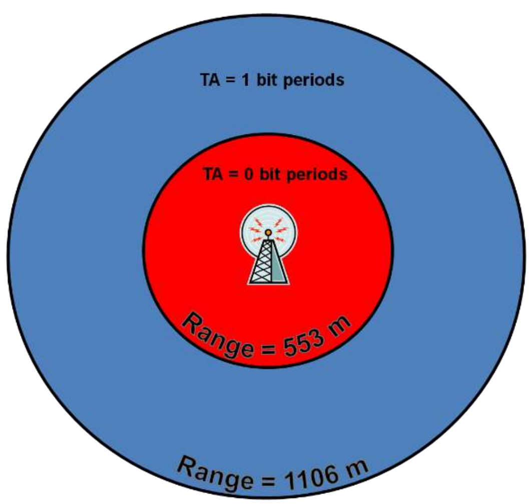


Figure 9: Ranges of Incremental Timing Advances

This Figure shows the area around a tower that would return a TA of zero (red) to the receiver corresponding to a range anywhere from 0 m to 553.46 m from the tower. Similarly a TA of one (blue) corresponds to a range from 553.46 m to 1106.92 m. This large area where the TA data will equal one discrete range value will create relatively large latitudinal and longitudinal errors compared to a GPS solution. But in the absence of GPS availability, several minutes of unaided dead reckoning operation can lead to kilometers of uncertainty. Thus the TA measurements from the cell phone signals will bound the errors on the navigation state and permit the aircraft to return home.

## 3.2 Software

The software consists of two cascaded filters. The first filter is the AHRS. The second is a dead reckoning filter.

### 3.2.1 AHRS Filter

The AHRS portion of the algorithm consists of a six state EKF. The states of the EKF includes the three Euler angles (roll angle, $\hat{\phi}$; pitch angle, $\hat{\theta}$; and heading angle, $\hat{\psi}$) as well as three gyroscope bias values($\hat{p}_{bias}$, $\hat{q}_{bias}$, and $\hat{r}_{bias}$) which correspond to the x, y, and z-axis rotation rate biases, respectively. The hat, "$\hat{}$" , indicates an *estimated* quantity. This filter employs gyro-integration for the time update prediction step described in Equation 2 where the subscript $k$ designates the current epoch and $k+1$ the next epoch.

$$\begin{bmatrix} \hat{\psi}_{k+1} \\ \hat{\theta}_{k+1} \\ \hat{\phi}_{k+1} \end{bmatrix} = \begin{bmatrix} \hat{\psi}_{k} \\ \hat{\theta}_{k} \\ \hat{\phi}_{k} \end{bmatrix} + \Delta t \begin{bmatrix} 1 & \sin\hat{\phi}_k \tan\hat{\theta}_k & \cos\hat{\phi}_k \tan\hat{\theta}_k \\ 0 & \cos\hat{\phi}_k & -\sin\hat{\phi}_k \\ 0 & \dfrac{\sin\hat{\phi}_k}{\cos\hat{\theta}_k} & \dfrac{\cos\hat{\phi}_k}{\cos\hat{\theta}_k} \end{bmatrix} \begin{bmatrix} p \\ q \\ r \end{bmatrix} \tag{2}$$

This update occurs at a 50 Hz rate.

The measurement update occurs at a rate of Hz and used to arrest the drift caused by gyro integration. The acceleration measured by the IMU in the body frame is corrected for aircraft centripetal acceleration and then is converted into the navigation frame using the body to navigation transformation matrix (denoted by $R_{B2N}$) given by the direction cosine matrix in Equation 3.

$$R_{B2N} = \begin{bmatrix} \cos\theta\cos\psi & \cos\theta\sin\psi & -\sin\theta \\ \sin\phi\sin\theta\cos\psi - \cos\phi\sin\psi & \sin\phi\sin\theta\sin\psi + \cos\phi\cos\psi & \sin\phi\cos\theta \\ \cos\phi\sin\theta\cos\psi + \sin\phi\sin\psi & \cos\phi\sin\theta\sin\psi - \sin\phi\cos\psi & \cos\phi\cos\theta \end{bmatrix} \tag{3}$$

The difference between this acceleration experienced by the aircraft and gravity serves as the innovation for the measurement update used to determine $\hat{\phi}$ and $\hat{\theta}$. The measurement update for $\hat{\psi}$ is calculated using magnetic field measurements from a magnetometer triad. The difference between the measured magnetic field in the body frame (converted to the navigation frame) and the local magnetic field of the given flight area is used as the innovation vector. This local magnetic field is hard-coded into the algorithm prior to flight using the World Magnetic Model (WMM) 2010.

### 3.2.2 Dead Reckoning Filter

The dead reckoning filter is an 11 state EKF. The 11 states consisted of:

1. Latitude ($\hat{\Lambda}$)
2. Longitude ($\hat{\lambda}$)
3. Altitude ($\hat{h}$)
4. North/South Wind Component $\hat{W}_{North}$
5. East/West Wind Component $\hat{W}_{East}$
6. Estimated Error on AHRS $\hat{\psi}$
7. Estimated Error on AHRS $\hat{\theta}$
8. Airspeed Measurement Error in X Component of Body Frame
9. Airspeed Measurement Error in Y Component of Body Frame
10. Airspeed Measurement Error in Z Component of Body Frame
11. Barometric Altitude Offset from Estimated Altitude ($\hat{h}$)

The time update stage of the filter was performed by projecting the body frame airspeed into the navigation frame, correcting for estimated wind, and using those estimated inertial velocities within the latitude, longitude, and altitude rate equations shown in Equation 4.

$$\begin{bmatrix} \dot{\Lambda}_k \\ \dot{\lambda}_k \\ \dot{h}_k \end{bmatrix} = \begin{bmatrix} \dfrac{\hat{V}_{North} + \hat{W}_{North}}{R_{NS} + \hat{h}} \\ \dfrac{\hat{V}_{East} + \hat{W}_{East}}{(R_{EW} + \hat{h}) * \cos(\hat{\Lambda})} \\ -\hat{V}_{Down} \end{bmatrix}] \tag{4}$$

Where $R_{NS}$ is the Earth's radius of curvature in the North/South direction, and $R_{EW}$ is the radius of curvature in the East/West direction. These rate equations were then used in Equation 5 to predict the 3-dimensional position of the aircraft at the next epoch where the $\hat{W}$ and $\hat{V}$ specify a wind estimate and a velocity estimate in the navigation frame respectively. In addition to this time update process, an altitude-based measurement update made use of an innovation derived from the difference in the measured barometric altitude and the estimated altitude, $\hat{h}$. This measurement update immediately follows the time update at the same rate of 50 Hz.

$$\begin{bmatrix} \hat{\Lambda}_{k+1} \\ \hat{\lambda}_{k+1} \\ \hat{h}_{k+1} \end{bmatrix} = \begin{bmatrix} \hat{\Lambda}_k \\ \hat{\lambda}_k \\ \hat{h}_k \end{bmatrix} + \Delta t \begin{bmatrix} \dot{\Lambda k} \\ \dot{\lambda}_k \\ \dot{h}_k \end{bmatrix} \tag{5}$$

Aiding measurement updates are provided by the cell phone TA data which are converted into range measurements, $\rho$, from each individual cell phone tower signal received by the onboard modem. In an effort to simplify the problem, a *library* of CIDs and their locations in the flight area were surveyed *a priori*. Although a method for estimating tower locations is feasible when GPS is available to the aircraft (using TA ranges to towers to reverse the problem from locating the aircraft to locating the tower as described in [11]), the 553.46 m range errors combined with the relative ease with which the towers were physically located made this method expedient. Therefore, with the locations of the towers known, the measurement update provided by TA ranges becomes very similar to a measurement update provided by GPS receiver ranges to satellites. Due to the large position errors inherent to the TA ranges, an update rate of 0.2 Hz was chosen instead of a 1 Hz update used in GPS-aided INS filters.

These measurements were completed by first converting the coordinates of the cell phone towers into Earth-Center, Earth-Fixed (ECEF) coordinates followed by converting into North, East, and Down (NED) coordinates from a common reference origin chosen to be the initialized location of the SUAV. During flight when GPS becomes unavailable, the estimated location of the aircraft is converted to the NED frame. Next, the observed CIDs and TA data is parsed to determine if a CID matches the library. Based upon the definition of timing advances given in [10], we assume the most likely range given by any TA data is exactly halfway between the measured bit period and the next. Therefore we add 0.5 to the rounded bit period returned as the TA and calculate the TA range as shown in Equation 6.

$$\rho\,(\mathrm{m}) = (\text{bit periods} + 0.5) * (553.46\,\mathrm{m}) \tag{6}$$

Viewed another way, it is assumed that a TA value of zero will signify a range of 276.73 m from the aircraft to the corresponding tower. Likewise for a TA of one, we'll use a range of 830.19 m, and consequently, the best-case scenario of any range measurement will have a true range error of $\pm$276.73 m assuming there is no additional sources of error on the measurement, i.e. multi-path effects, etc. If a match between a received CID and the library occurs, the TA range is compared to the estimated range, $\hat{\rho}$, the aircraft is from the CID in question (calculated by Equation 8).

$$\hat{\rho}\,(\mathrm{m}) = \sqrt{(N_{SUAV} - \hat{N}_{CID})^2 + (E_{SUAV} - \hat{E}_{CID})^2 + (D_{SUAV} - \hat{D}_{CID})^2} \tag{7}$$

$$\begin{bmatrix} \mathrm{N}\ (\mathrm{m}) \\ \mathrm{E}\ (\mathrm{m}) \\ \mathrm{D}\ (\mathrm{m}) \end{bmatrix} = \begin{bmatrix} \dfrac{\hat{N}_{SUAV} - N_{CID}}{\hat{\rho}} \\ \dfrac{\hat{E}_{SUAV} - E_{CID}}{\hat{\rho}} \\ \dfrac{\hat{D}_{SUAV} - D_{CID}}{\hat{\rho}} \end{bmatrix} \tag{8}$$

Thus, the innovation is given by Equation 9 as the measured range subtracted from the estimated range.

$$\text{TA innovation (m)} = \rho - \hat{\rho} \tag{9}$$

One important note regarding the CID is that all CIDs observed in the flight area were 5 digit numbers where the first four digits corresponded to that unique cell phone tower. The fifth and final digit designated which *sector* the signal was being received by. Each CID observed consisted of three possible sectors located in an equilateral triangle around the tower or structure. This is illustrated in Figure 10 where the cell phone tower is 1234 and the sectors are 1, 2, and 3. This arrangement could create the situation whereby the +CCED command returned TA data for each of the three sectors, two of the three, or just one. Thus in the case where multiple TA ranges were reported for the same tower, the backup system would implement a measurement update only on the TA range that was the smallest of the group. This was done because test data showed that typically the shortest TA range corresponded to the sector antenna that was most directly oriented at the receiver at the time the +CCED command was requested. The other sectors typically returned larger TA values most likely due to multi-path given the indirect path the signal must take to "wrap" around the tower and be received by a sector not directly pointing at the SUAV.

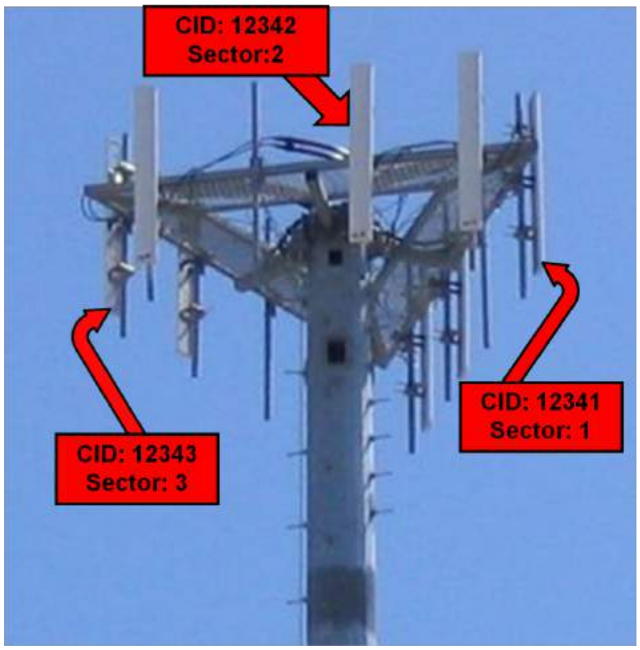


Figure 10: Sector Arrangement for Hypothetical Cell Phone Tower 1234

Another important check prior to fully completing any TA range update was an inspection of the innovation compared to the expected innovation covariance. Figure 12 shows a subset of 160 TA ranges and corresponding true ranges (derived from GPS data) to a particular cell tower. The TA range compares as expected, $\pm 553.46\,\mathrm{m}$, to the true ranges from the towers except for a few "spikes" particularly evident on the left side of the figure. The errors are shown on the figure and are considerably higher than $553.46\,\mathrm{m}$. These spikes are believed to be due to multi-path effects because of there increased frequency when the cell phone receiver is closer to the ground where trees, buildings, etc. can obstruct line-of-sight (LOS). In order to prevent these faulty TA ranges from corrupting the solution, the standard deviation of the innovation, $\sigma_{innov}$, is calculated by taking the square root of the innovation covariance defined by [12]. A cutoff multiplication factor of 1.5, i.e. $1.5 * \sigma_{innov}$, is used and this value is compared to the innovation calculated during each measurement update as defined in Equation 9. The multiplication factor of 1.5 was settled upon empirically after several experiments were conducted using a variety of multiplication factors.

The effectiveness of this method relies upon accurate statistical models for the process noise, $Q$, of the time update and measurement noise, $R$, of the aiding update. Additionally, the state errors due to process noise must grow at a sufficiently slow pace to keep the innovation covariance small enough to expect relatively small innovations. Otherwise, the errors due to process noise of the time update will increase the covariance, $P$, so quickly that large innovations are expected and thus it will be difficult to differentiate the inaccurate measurements from the accurate ones. Despite the low-cost sensors used in the SUAV, the covariance of the dead reckoning filter does in fact grow at a slow enough rate, and using a measurement noise of $R = 553.46\,\mathrm{m}$, the method of comparing $1.5 * \sigma_{innov}$ to the measured covariance does an exceptional job of rejecting the spikes of inaccurate TA measurements. Figure 11 demonstrates this where the innovation is plotted along side the $1.5 * \sigma_{innov}$ for one particular CID observed during one flight test. As seen in Figures 11 and 12, the spikes are relatively rare with the majority of the TA ranges being around the expected value (as is the case in Figure 11) and near the true range (in Figure 12).

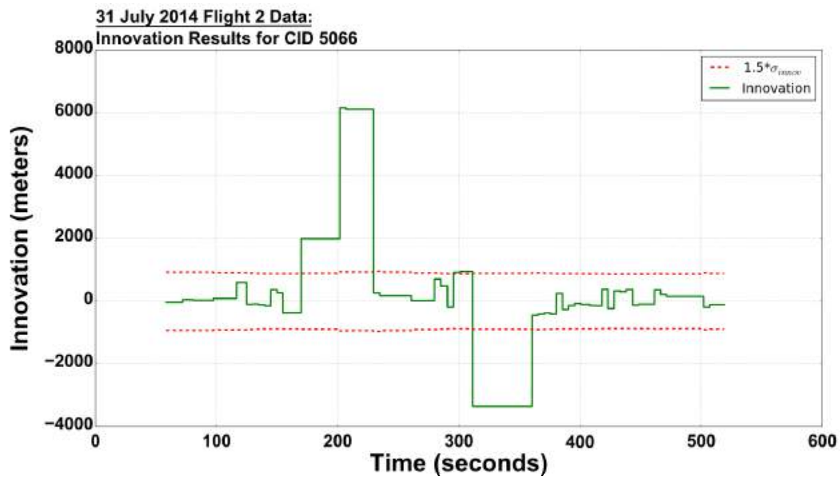


Figure 11: TA Range Innovation vs. Inaccurate Innovation Cutoff

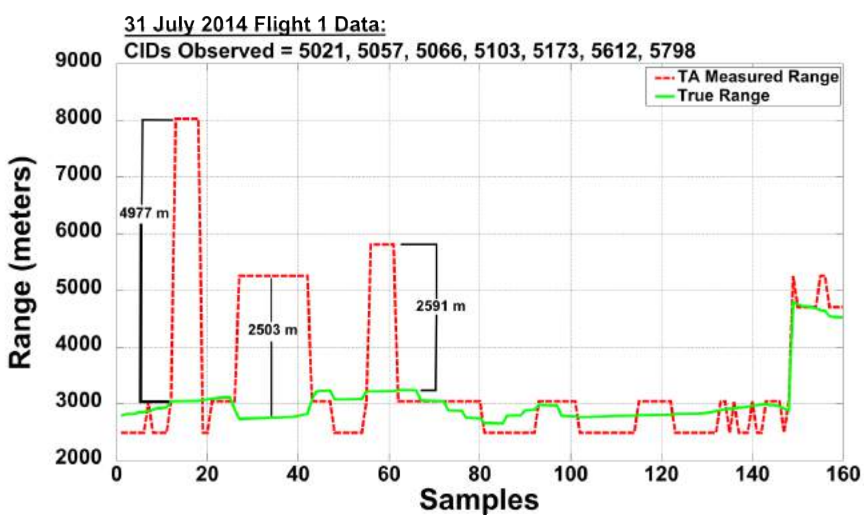


Figure 12: Cell Phone TA Range vs. True Range

Other logic checks included a barometric altitude check and GPS outage determination. The altitude check was introduced due to multi-path effects noticed when the aircraft was below the tree-line. These multi-path effects would create erroneous measurements yielding TA ranges that were on the order of 2 to 6 times larger than the true distance (similar to the spikes shown in Figures 12 and 11) with the exception that they were much more frequent when close to the ground. An altitude threshold of 10 meter above ground level (AGL) was settled upon. That is TA measurements are ignored when the UAV is less than 10 meters above the ground. The GPS outage determination consisted of a simple check to see if the GPS receiver was reporting new measurements every second. If there was no new data for at least two consecutive seconds, the backup system was enabled.

# 4 System Performance

Both flight testing and hardware-in-the-loop (HIL) simulations were performed to analyze the effectiveness of the cell phone-aided dead reckoning system. In both cases, a *reference* GPS-aided INS filter was used to determine the true navigation state of the aircraft. In order for this reference filter to accurately determine the navigation state, a continuous and uncorrupted stream of 1 Hz GPS data has to be supplied to it by the Hemisphere Crescent OEM board. This reference filter and the required GPS data was run in the background of the flight-code that controlled and operated the aircraft, thus preventing any interaction between the backup system and the GPS-aided filter. The GNC algorithms that guided and controlled the aircraft throughout the flights and simulations were supplied with a navigation solution determined by the cell phone-aided dead reckoning system.

All flight testing was conducted at the University of Minnesota Outreach, Research and Education Park (UMore Park) located near Rosemount, MN. Our cell phone modem, the Multi-Tech Systems MT100EOCG-G2, was equipped with a T-Mobile network Subscriber Identity Module (SIM) card. Therefore, the onboard cell phone receiver was capable of communicating with T-Mobile network cell phone towers within LOS of the UMore Park flight area. To develop the "library" of CIDs, the authors gathered the position information on sixteen T-Mobile towers. These cell phone tower locations in addition to the flight area are shown in Figure 13.

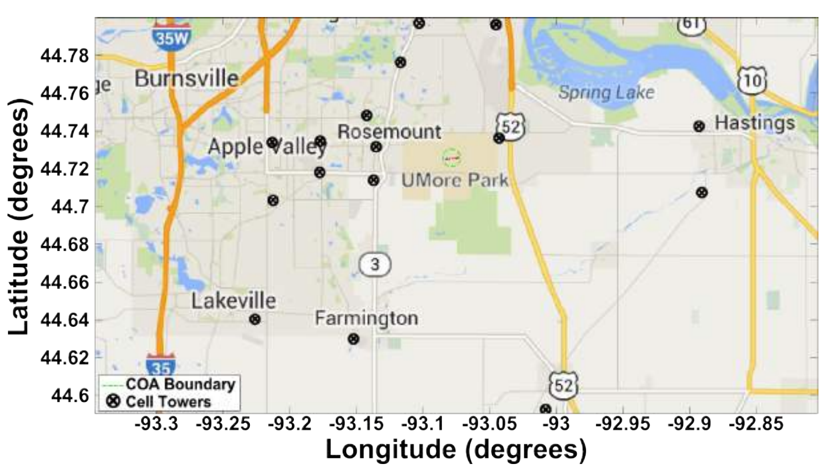


Figure 13: UMore Park Flight Area & Known Cell Tower Locations

Figure 14 displays a close-up of the UMore Park flight area depicted in Figure 13 in NED coordinates as well as the boundaries of the Certificate of Authorization (COA) obtained by the UMN-URG from the Federal Aviation Administration (FAA) authorizing SUAV operations within the area designated by the green dashed circle. The COA is a certification of operations which includes the ground station, airframe, and operating procedures. The ground station and airframe used in a flight test conducted on 31 July 2014 are shown in Figures 15 and 16.

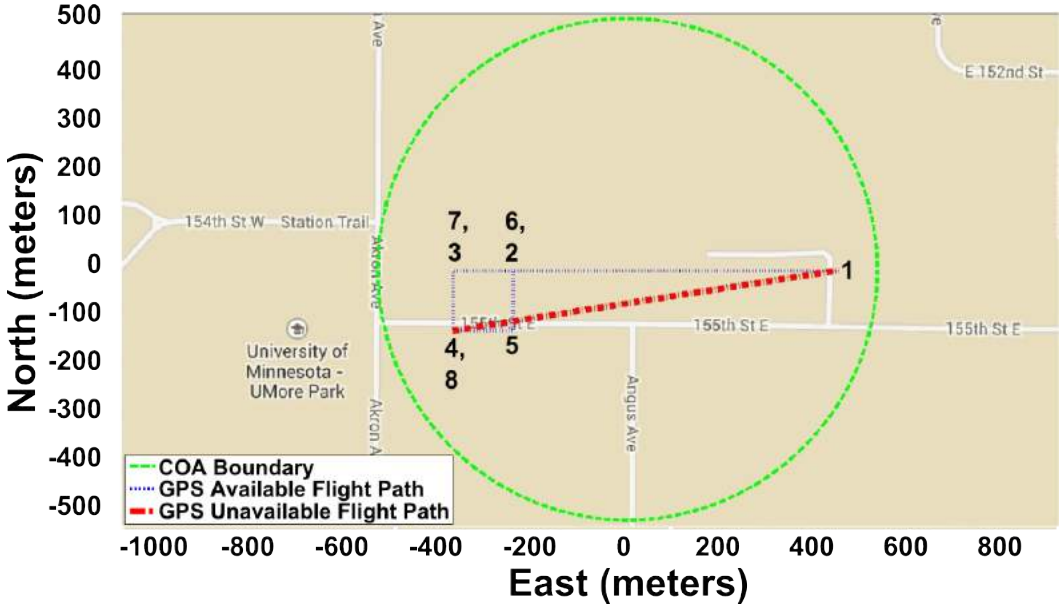


Figure 14: UMore Park COA and Pre-Programmed Flight Path for Testing

Figure 15: Flight Test Setup

Figure 16: Ultra Stick 25e in Flight

The pre-programmed route loaded into the SUAV flight-code prior to each flight is shown in the middle of the COA. This route was flown completely autonomously by the SUAV during the flight tests and the first set of HIL simulations. The sequence of way-points are indicated by the numbering (with way-point 1 being "home" and way-point 8 being the GPS outage start point), and the dotted blue line indicates the portion of the flight when GPS is available. This portion of the flight replicates the CONOP presented in Section 2 and Figure 4. The dash-dotted red line indicates when GPS becomes unavailable and the backup system is enabled to demonstrate the CONOP detailed in Figure 5.

## 4.1 Flight Test Results

As illustrated in Figure 14, the size of the COA boundaries only allow for a 1100 m radius centered at 44°43′32.71″ N and 93°4′44.49″ W. This fact coupled with the measurement noise on the TA ranges containing an inherent error of 553.46 m means that it is difficult to observe large corrections caused by the cell phone-aiding. Stated another way, the terms of the COA prevent test flights that include a long enough straight-line path to allow the drift from the dead reckoning time update to exceed the measurement noise of 553.46 m. This is reflected in the flight test data shown in Figure 17.

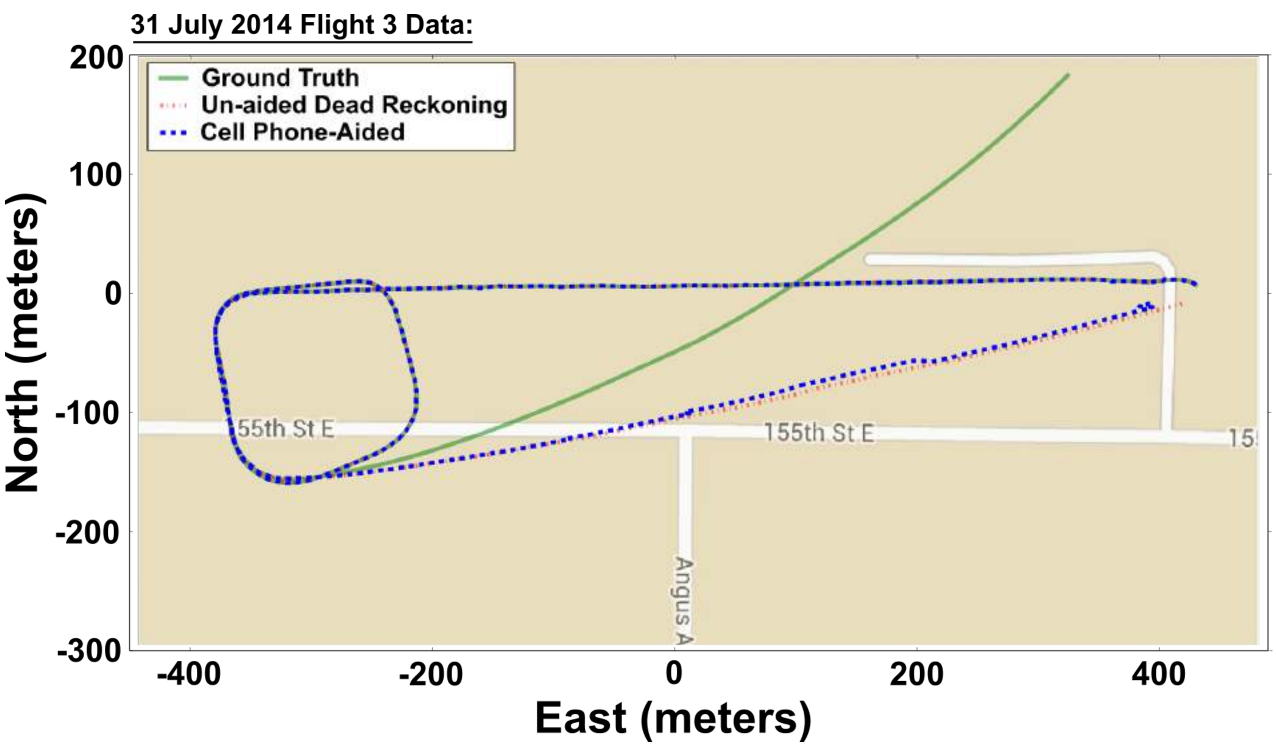


Figure 17: Flight Test: Comparison of Position Solutions

This plot shows the results of one flight test with the position solutions for three filters. The reference (ground truth) is shown in green. The un-aided dead reckoning (time update only with no measurement updates) displayed in red, and the cell phone-aided dead reckoning (with measurement updates provided by cell phone TA data) outlined in blue. By design, all three filters provide the same solution during the portion of the flight when GPS is available as evidenced by the pre-programmed flight plan shown in Figure 14. However once way-point 8 is passed, a GPS outage is simulated. Subsequently, the aircraft heads back home without GPS available. The un-aided dead reckoning and cell phone-aided dead reckoning filters direct the aircraft at a heading that they estimate will get the SUAV back home. Nevertheless as indicated by the green ground truth, the aircraft is actually drifting to the north of the estimated path that will return it home. Despite this drift, small adjustments can be seen in the estimate of the cell phone-aided dead reckoning filter, and these adjustments *pull* the aircraft's ground truth to the south effectively correcting the solution and reducing the position error. This behavior is not seen in the un-aided dead reckoning filter due to the absence of any measurements to correct the drift. Figure 18 displays this result in another way. The 3-Dimensional position error magnitude is plotted against time starting at the moment GPS becomes unavailable. It is clear from this plot that the errors on the cell phone-aided dead reckoning filter are less than those experienced by the un-aided dead reckoning filter due to the fusion of TA range estimates into the solution.

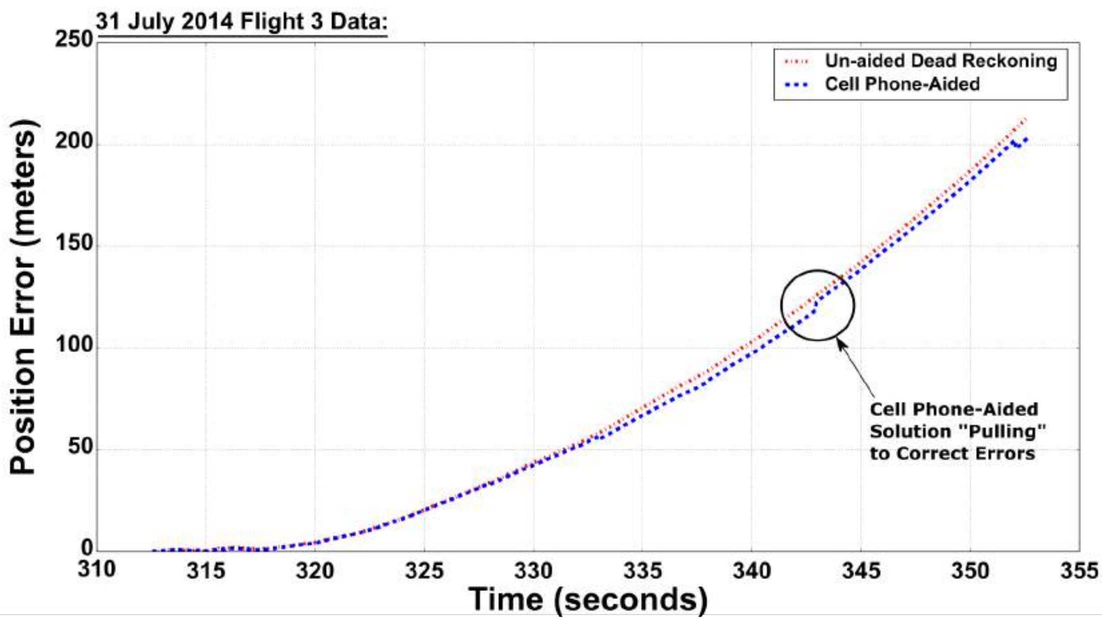


Figure 18: Flight Test: Comparison of Position Error Growth

Additionally as noted in Section 2, the backup system provides an altitude estimate with small errors as shown in Figure 19. This is due to the continued aiding of the vertical channel by the barometric measurement updates provided by the pitot-static system. The ability of the cell phone-aided dead reckoning system to consistently track the true altitude with small errors over a sustained GPS outage will be further demonstrated later in this report when the HIL simulation is discussed.

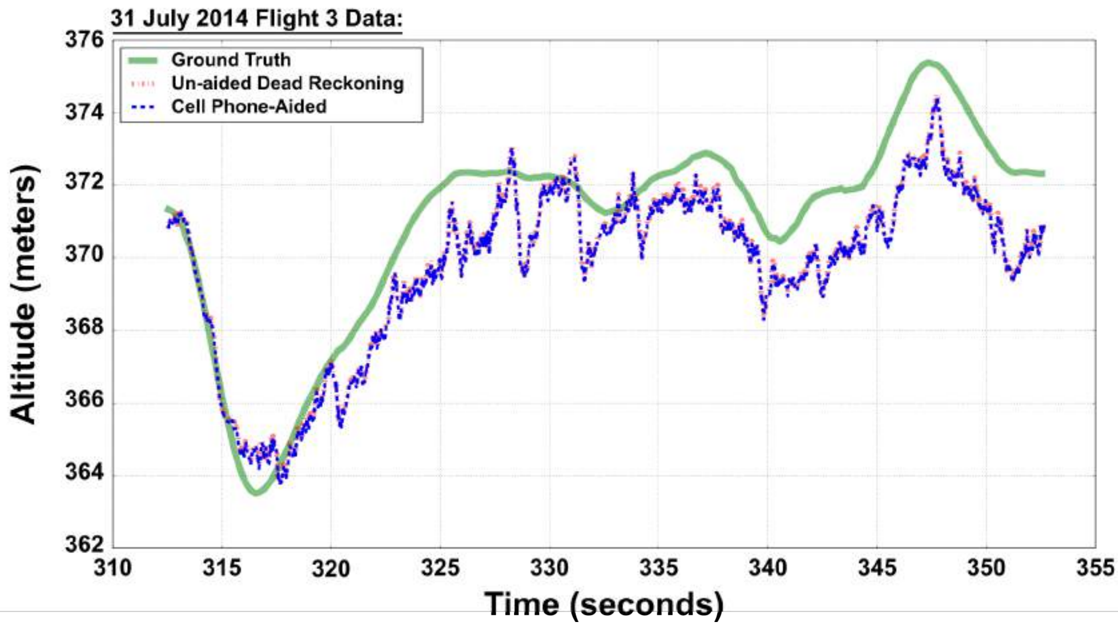


Figure 19: Flight Test: Comparison of Altitude Estimates

## 4.2 Simulation Results

As noted earlier due to the limited airspace available within the COA area for flight testing, the performance of the cell phone-aided dead reckoning system during a persistent GPS outage experienced over the course of several miles was not assessed (by the method of flight testing). However, we were able to make use of the UMN-URG Hardware in the Loop (HIL) simulation environment to mimic the conditions experienced during flight testing to evaluate the effectiveness of the cell phone-aided dead reckoning filter during long periods of GPS outages. Figure 20 shows a schematic of the HIL depicting signal flows and modules.

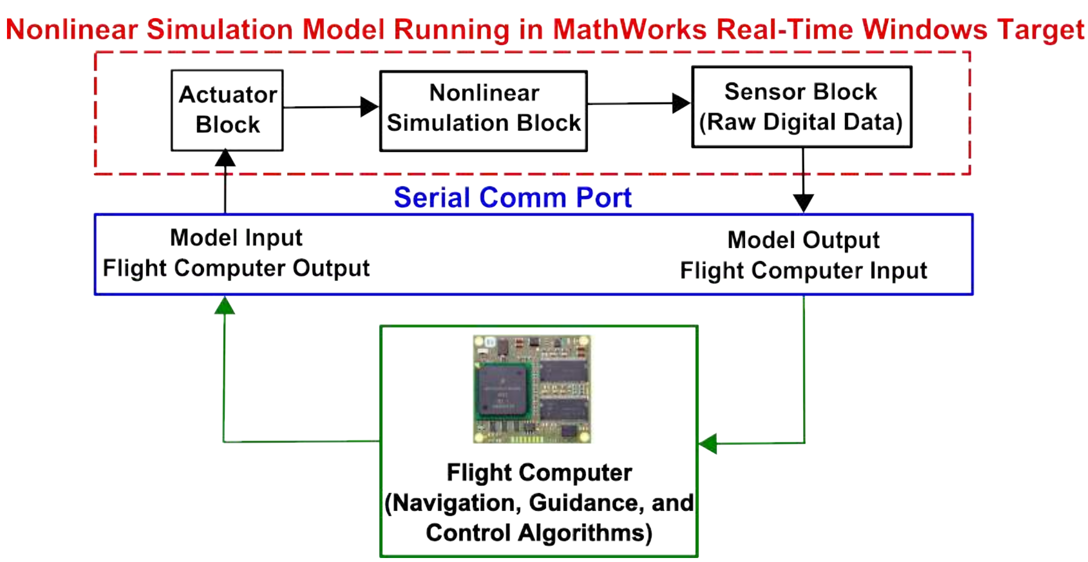


Figure 20: Hardware-in-the-Loop Simulation Block Diagram

This HIL simulation utilized a 6 degree-of-freedom (DOF) nonlinear simulation model created in MathWorks Simulink to accurately compute the aircraft dynamics during flight. The model is equipped with the aircraft's full nonlinear equations of motion, aerodynamics, and propulsion models derived from wind-tunnel testing to accurately represent the dynamics of the Ultra Stick 25e aircraft. Additionally, the simulation included models for relevant SUAV subsystems such as the actuators, motor, propeller, and sensor dynamics for the IMU, pitot-static system, and GPS including noise characteristics. An environmental model was used to recreate Earth's atmosphere, gravity, magnetic field, wind, and turbulence. MathWork's Real-Time Windows Target toolbox was used to ensure the simulation runs in real time on a Windows PC in order to supply the Goldy FCS flight computer with simulated sensor data at the required 50 Hz rate [13]. Figure 21 depicts the physical setup during a HIL simulation.

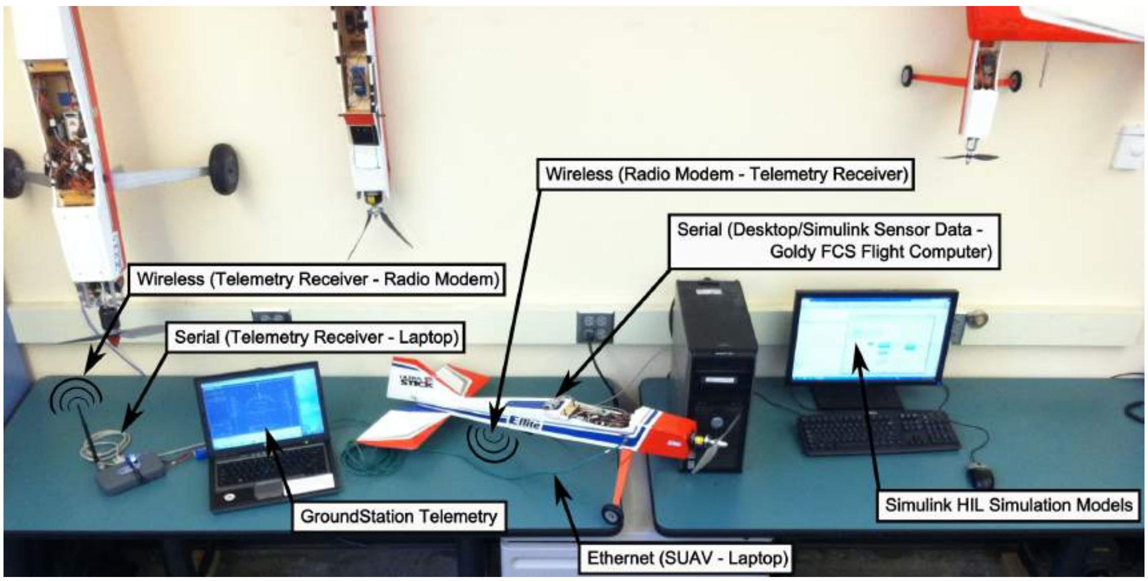


Figure 21: Hardware-in-the-Loop Simulation Setup

To assure the HIL simulation results obtained are representative of those that would have been collected during real flight testing, accurate sensor error models were developed. With respect to the cell phone modem, this was done by collecting TA data from several flight tests and constructing a probability density function. The TA ranges were simulated in MathWorks Simulink by first determining the true range from each of the sixteen cell phone towers to the aircraft given the cell phone tower locations and true aircraft position (determined by 6 DOF nonlinear Ultra Stick 25e model) are known. During flight testing, the +CCED command will return the TA data for the serving cell phone tower and up to six neighboring cell phone towers depending upon whether those additional six towers have LOS communication with the onboard cell phone modem. To replicate this behavior, the number of LOS cell phone towers available at the measurement epoch, $n$, was randomly chosen from a uniform discrete distribution between 1 and 7. Then $n$ closest tower CIDs and corresponding true ranges were selected for the simulated sensor data. Finally, the true range to each tower was corrupted by noise and converted into a TA corresponding to the rounded bit period as described in Section 3 by Equation 10.

The *noise* value was chosen by randomly selecting a value based on a normal distribution with zero mean and a standard deviation of 350 m. This distribution was determined experimentally as described earlier. This error distribution is shown in Figure 22 which displays the ranging error of the HIL simulated TA data based upon $\bar{\rho} - \hat{\rho}$ where $\bar{\rho}$ is the true range and $\hat{\rho}$ is the range measurement from TA data. For verification, this simulated error distribution compares well with that obtained from real flight data shown in Figure 23. As expected, the flight data error distribution exhibits the large spikes (outliers) discussed earlier. However since the backup system employs a check on the expected innovation using the $1.5 * \sigma_{innov}$ factor, the spikes were not simulated. Nevertheless, both plots depict similar behavior in the core of the probability density function indicating that the simulation reasonably imitates real-world TA data.

$$\rho = \text{round}\left[\frac{\bar{\rho} \pm noise}{553.46\,\text{m}}\right] \text{for } 1 \leq n \leq 7 \tag{10}$$

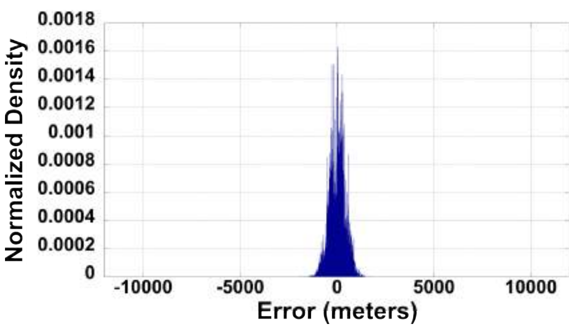


Figure 22: HIL Simulated TA Ranging Error Distribution

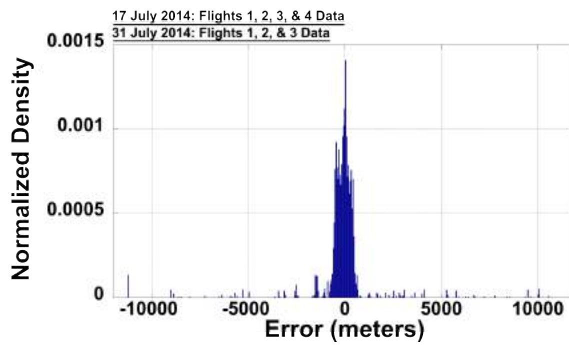


Figure 23: Flight Data TA Ranging Error Distribution

Another important factor addressed to ensure the simulation results reflect real flight testing was wind conditions. The environmental model winds were set to match the winds experienced during the flights that generated the plots shown in Figures 17 - 19. The winds on the day of flight testing were generally light and variable with periods of a sustained speed of $5\,kts$ wind from the South. This observation was reflected in the estimates of the north and east wind states in the dead reckoning filter which approximated that the steady wind varied from $0.5\,m/s$ ($0.97\,kts$) to $4.25\,m/s$ ($8.26\,kts$) with a turbulence of $0.5\,m/s$. The Low-Altitude Discrete Dryden Wind Turbulence Model from the MathWorks Aerospace Blockset was used in the HIL simulation, and the turbulence was set to $0.5\,m/s$ on all three body axes. In order to duplicate the northern drift displayed in Figure 17, the steady wind was set to $0.5\,m/s$ and ramped up to $4.25\,m/s$ midway through the simulated flight.

With the simulation models set, the flight computer was loaded with the same GNC software used during the flight tests and produced the results summarized in Figure 24 which shows a very similar pattern of the position solutions as that seen in the flight test results plotted previously in Figure 17. With this validation and verification of the HIL simulation, we proceeded to simulate an extended GPS outage occurring over the course of several miles.


Figure 24: HIL Simulation: Comparison of North and East Estimated Positions

For the lengthened flight path used during this HIL simulation, a start point was chosen at the western most edge of the known cell tower coverage area. This point was chosen for the ability to simulate an eastbound flight path that would traverse the entirety of the tower coverage. This start point was located near Apple Valley, MN, and normal operations (i.e. GPS available) are being conducted near this point at the beginning of the simulation. The SUAV home base was chosen 14 miles to the east near Hastings, MN. When GPS services are interrupted, the SUAV will attempt to navigate to this home base. This simulation was completed using the full library of sixteen cell phone towers within a 235.19 $squaremile$ area creating a cell phone tower density of 14.7 $square\,mile/tower$.

Figures 25 and 26 show the results generated during one extended simulation. Figure 25 shows the desired flight path in green which designates the course each filter attempts to track. The red and blue line represent the ground truth of the SUAV when navigated by the un-aided dead reckoning filter and cell phone-aided dead reckoning filter respectively. As indicated by the error plot in Figure 26, the un-aided dead reckoning solution drifts to the south and leads the ground truth by a considerable amount over the course of the 14 mile route causing western errors as well. This data clearly displays the effect of the TA measurements have on the position error when compared to an open loop un-aided dead reckoning solution. After completing three Monte Carlo simulations, the average position error of the un-aided dead reckoning solution was to 6765 m compared to a 200 m error on the cell phone-aided dead reckoning filter. Finally, the altitude estimate from both the cell phone-aided dead reckoning filter and open-loop dead reckoning filter maintains sub-meter accuracy as shown by Figure 27. This is due to continuous barometric measurement updates provided by the pitot-static system in each filter.


Figure 25: Extended HIL Simulation: Comparison of North and East Estimated Positions

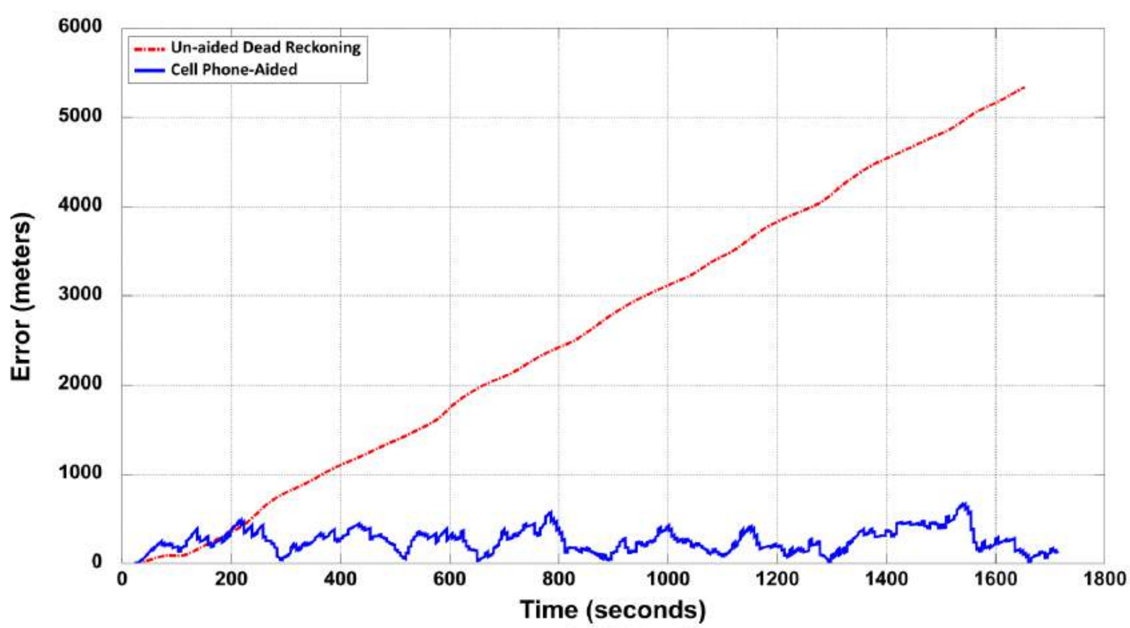


Figure 26: Extended HIL Simulation: Comparison of Position Error Growths

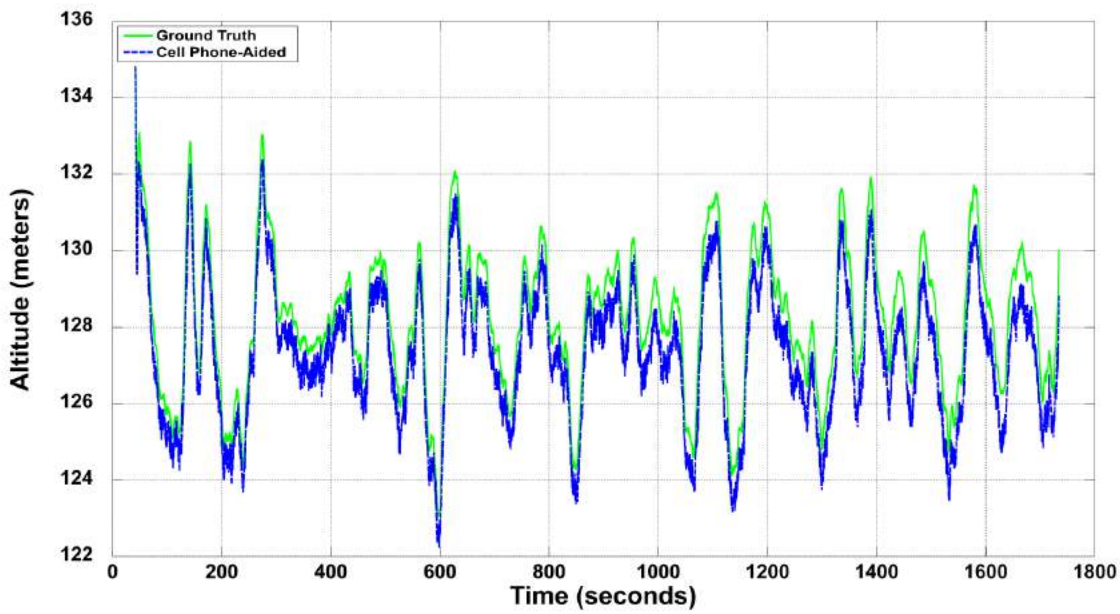


Figure 27: Extended HIL Simulation: Comparison of Altitude Estimates

# 5 Conclusion

In this work, we have demonstrated that a SUAV flight control system equipped with an airspeed-based dead reckoning filter can be aided by TA range measurements derived from cell phone signals to provide a navigation solution when GPS is unavailable. It was shown that this system can safely return the SUAV to its home base (or other unaffected region) when a GPS interruption occurs. With current COTS equipment, range measurements to cell phone towers are limited to a 553.46 m accuracy. However, this is sufficient to provide a measurement update capable of bounding the large drift errors inherent to un-aided dead reckoning navigation filters that make use of low-cost COTS IMUs.

The multilateration technique used in this system requires knowledge of cell phone tower locations in the SUAV flight area before flight. Currently most cell phone network providers are reluctant to provide the precise coordinates of their towers. Consequently, for this work, a list of relevant CIDs in communication with an onboard cell phone modem was developed from ground test data. Then this list was cross-referenced with databases from publicly available application programming interfaces (APIs) for cell phone tower locations to verify their approximate positions. Although feasible for research purposes, this method may be too labor intensive for real-world applications. For these uses, cell phone tower locations may need to be determined by an additional estimation algorithm designed to determine tower positions while GPS is available. Alternatively, perhaps a more accurate and computationally faster method would be to incentivize network providers to make their tower locations available to users (possibly via encryption). This would also reduce memory requirements in the low-cost COTS flight computers of SUAVs by no longer needing hard-coded *libraries* of expected CIDs. It can be reasonably assumed that the cell phone towers have position information available due to the fact that Time of Day information is provided to the towers and network by GNSS and/or GPS receivers [14].

This reliance upon GNSS and/or GPS receivers for critical time information would seem to create a liability for the cell phone-aided dead reckoning system (which is reliant upon network clocks to calculate TAs), and as reported by [4], GPS outages have interfered with cell phone networks due to the network's reliance upon GPS time for synchronization and calculations. However, network providers have recognized the vulnerabilities of GPS and are addressing the issue. Legacy equipment that previously provided base stations with frequency synchronization are being decommissioned, and equipment that rely on GPS for Time of Day information are being upgraded with IEEE1588 Precision Time Protocol (PTP) for a more robust time synchronization process between base stations and mobile users [14]. In addition to GPS vulnerabilities, these upgrades are also being motivated by Federal Communications Commission requirements of wireless carriers to provide latitude and longitude of callers in 9-1-1 emergencies. The accuracy standards of these requirements are 50 m to 300 m translating to 150 ns timing accuracies even for callers within buildings where GPS is unavailable thus requiring an improved time synchronization protocol. Therefore, with these improvements to carrier networks, we believe that the TA data needed for the backup system will be available during GPS interruptions.

# 6 Future Work

Despite this backup system proving the concept of using cell phone signals to aid an airspeed based dead reckoning filter, 553.46 m position errors are very large especially for SUAVs in particular. One of the utilities of these small aircraft is to perform operations at lower altitudes and in tighter spaces, and although a backup system will not be as accurate as GPS, it is desired that the backup will allow the SUAV to exit any GPS-denied region safely including urban settings containing many obstacles within tens of meters. This research proves a multilateration approach using cell phone signals can be implemented into a SUAV flight control system. However, further research using a software defined cell phone modem may lead to improved system performance. This will require receivers that can make measurements that reduce the granularity of the rounded bit period TAs. Currently, such receivers do not exist. One can be implemented as a software defined redio. In the short term, this migration away from COTS equipment may increase costs. However, evolving technology in the clock industry has allowed for the development of chip-scale atomic clocks with single unit quantities having comparable cost to other low-cost SUAV autopilot components at $1500 [15]. Consequently, an advanced cell phone modem equipped with a highly accurate atomic clock can still comply with the low-cost nature of SUAV components while providing a considerable increase in accuracy.

Additionally, an intelligent integration of RSSI into an estimation filter may increase location accuracy. Although not as accurate as direct measurement of the signal TOA, the signal strength (as measured by RSSI) may serve as an indirect evaluation of range from the modem and cell phone tower, or perhaps a more promising usage would be RF fingerprinting. A brief examination of RSSI was conducted during the course of this work, and patterns in RSSI were evident with stronger signals received when the SUAV was closer to the corresponding cell phone tower. The patterns seemed to be more predictable and consistent with stronger signal strengths indicating improved performance when the tower is relatively close to the flight area. Additionally, the SUAV used for this testing employed one cell phone antenna which was subject to having the received signal blocked and/or interfered with by the aircraft itself. Thus multiple antennas strategically placed on the SUAV may prevent interference and consequently provide optimal measurements for determining RSSI trends based on aircraft location.

Finally, the effectiveness of using cell phone signals for localization needs to be evaluated for all the settings that SUAVs will be deployed in. For instance, an evaluation is needed for what role cell phone tower density has on the performance of these systems, such as the one presented in this paper as well as those proposed for future exploration. This will be particularly relevant for rural settings like those encountered in border patrol operations or agricultural applications where tower coverage is more sparse than urban areas. Likewise a reduced tower coverage may be experienced during CONOPs that may require non-line-of-sight (NLOS) communications for cell phone modems, i.e. indoor operations. One possible solution for NLOS environments was presented in [16] where signal time of arrival, angle of departure, and the Doppler shift are used for localization with a demonstrated accuracy of 10 cm in 75% of the cases for sufficiently high Signal-to-Noise Ratio (SNR).

# References

[1] Demoz Gebre-Egziabher and Brian Taylor, 2012, *Impact and Mitigation of GPS-Unavailability on Small UAV Navigation, Guidance and Control*, Report #2012-2, University of Minnesota, Department of Aerospace Engineering and Mechanics, November 2012

[2] Army UAS CoE Staff, *Eyes of the Army: US Army Roadmap for Unmanned Aircraft Systems 2010-2035*, US Army UAS Center of Excellence (ATZD-CDI-Q), Fort Rucker, AL, 2010. pp.12.

[3] Honeywell Inc. (2011). *Honeywell T-Hawk Aids Fukushima Daiichi Disaster Recovery*[Press Release]. Retrieved from http://honeywell.com/News/Pages/Honeywell-T-Hawk-Aids-Fukushima-Dai ichi-Disaster-Recovery.aspx

[4] Evans-Pughe, C. (2011, April). GPS vulnerability to hacking. *Engineering & Technology Magazine*, 6(4), Retrieved from http://eandt.theiet.org/magazine/2011/04/gps-vulnerabilities.cfm?origin=EtOtherStories

[5] Marks, P. (2012, May). GPS loss kicked off fatal drone crash. *New Scientist Magazine*, Retrieved from http://www.newscientist.com/blogs/onepercent/2012/05/gps-loss-kicked-off-fatal-dron.html

[6] University of Texas at Austin Aerospace Engineering and Engineering Mechanics. (2012). *Todd Humphreys' Research Team Demonstrates First Successful GPS Spoofing of UAV*. [Press Release]. Retrieved from http://www.ae.utexas.edu/news/features/todd-humphreys-research-team-demonstrates-first-successful-gps-spoofing-of-uav

[7] Z. Li and D. Gebre-Egziabher, *Performance Analysis of a Civilian GPS Position Authentication System*, Proceedings of IEEE/ION PLANS, Myrtle Beach, S.C. April 2012. pp.1028 - 1041

[8] A. M. Murch and Y. C. Paw and R. Pandita and Z. Li and G. J. Balas,*A Low Cost Small UAV Flight Research Facility*, 1st CEAS Specialist Conference on Guidance, Navigation, and Control, April 2011

[9] *Open Communications Gateways - Embedded*. MT100EOCG-G2. Rev. 86002160. Multi-Tech Systems Inc. August 2013.

[10] European Telecommunications Standards Institute (ETSI), *Digital cellular telecommunications system (Phase 2+); Radio subsystem synchronisation (GSM 05.10)* GSM Technical Specification 05.10 Version 5.0.0. Ref: TS/SMG-020510Q, (May 1996).

[11] Matti Raitoharju, Simo Ali-Lytty, and Lauri Wirola. *Estimation of Base Station Position Using Timing Advance Measurements*. Proc. SPIE 8285, International Conference on Graphic and Image Processing (ICGIP 2011), 82855L (September 30, 2011); doi:10.1117/12.913427.

[12] Simon, Dan. *Optimal State Estimation: Kalman, $H_\infty$, and Nonlinear Approaches*. Hoboken: John Wiley & Sons, Inc., 2006, Print.

[13] University of Minnesota UAV Laboratories. (July 2014). *Infrastructure: Aircraft Simulation*. Retrieved October 2014, from http://www.uav.aem.umn.edu/wiki/Infrastructure/AircraftSimulation

[14] Vitesse Semiconductor Corporation. *Precise Timing for Base Stations in the Evolution to LTE* California: Camarillo, 2013. Print

[15] Turley, J. (2011, November). Does Anybody Really Know What Time It Is?: Atomic Clocks for the (Almost) Everyday Embedded Designer. *Electronic Engineering Journal*, Retrieved from http://www.eejournal.com/archives/articles/20111116-symmetricom/

[16] K. Papakonstantinou and D. Slock, *Hybrid TOA/AOD/Doppler-Shift Localization Algorithm for NLOS Environments*, IEEE. pp. 1948 - 1952. - 1041